Inorg. Chem. **2009**, *48*, 1524−1532

A Magneto-Structural Study of a Hexanuclear $(V^{IV}{=}O)_6$-Complex and a Tetranuclear Mixed-Valent $[V^{III}_2V^{IV}_2]$ Species

Biplab Biswas, Thomas Weyhermüller, Eckhard Bill, and Phalguni Chaudhuri*

Max-Planck-Institut für Bioanorganische Chemie, Stiftstraβe 34-36, D-45470 Mülheim an der Ruhr, Germany

Received September 26, 2008

Syntheses, crystal structures, and magnetic properties are reported for a hexametallic and a mixed-valent tetrametallic vanadium cluster, namely $[Na(L^1)_6(V^{IV}{=}O)_6]ClO_4$ (**1**) and $[(L^2)_2V^{III}_2V^{IV}_2(\mu\text{-}Cl)_6Cl_4]$ (**2**), where H_2L^1 represents *N*-methyldiethanolamine and H_2L^2 *N*′*N*′-di(3,5-di-*tert*-butyl-salicylidene)-1,3-diaminobenzene. The structure of the cation in **1** is comprised of a hexagon of six $(V^{IV}{=}O)$ units, in which a sodium ion is encapsulated in the center of the hexagon. Thus, the hexametalate ring contains six d^1 ions, each of which is in an octahedral environment of O_5N atoms. Magnetic studies reveal the cluster to exhibit ferromagnetic exchange interactions ($J = +16.7 \pm 0.3$ cm^{-1}), which is rationalized by the orthogonal neighboring *xy* planes of d^1 $V^{IV}{=}O$ ions. The structure of complex **2** can be considered as two mixed-valent face-sharing bioctahedral units of $[V^{III}(\mu\text{-}Cl)_3V^{IV}]$ bridged by two *m*-phenylene linkers. The $V(1)^{III}\cdots V(2)^{IV}$ distances of av. 3.10 Å preclude metal−metal bonding. Variable-temperature magnetic susceptibility data are fitted to obtain the parameters $J_1 = -47.6$ cm^{-1}, $J_2 = +1.5$ cm^{-1}, $g(V^{III}) = 1.95$, $g(V^{IV}) = 1.85$ ($\hat{H} = -2J \times S_i \cdot S_j$). The ferromagnetic coupling J_2 operates at a distance of ∼7.09 Å between two vanadium centers through the spin polarization mechanism due probably to the topology (1,3-substitution) of the *m*-phenylene bridges. The X-band electron paramagnetic resonance (EPR) spectrum analyzed with $S_t = 1$ shows that the mixed-valent $V^{III}V^{IV}$ species has indeed been formed and the tetranuclear core remains intact in solution. The hyperfine coupling constants indicate the localized mixed-valence nature of **2**.

Introduction

The coordination chemistry of vanadium[1] is relevant to the bioinorganic chemistry of marine organisms and the insulin-like activity of oxidovanadium (V and IV) compounds; it is dominated mainly by three oxidation states: +V, +IV, and +III. V(III) ($3d^2$, $S = 1$) chemistry[2] is relatively less explored, due to a lack of suitable starting materials which can be handled under normal laboratory conditions and the pronounced tendency of the trivalent state to undergo oxidation. The recent noteworthy observation that tetranuclear vanadium(III) complexes with a butterfly structure behave as single-molecular magnets[3] motivated us to gain a better understanding of the electronic structure of multinuclear V(III) systems. Hence, we were prompted to synthesize polyvanadium paramagnetic complexes, which are the major thrust of our present work.

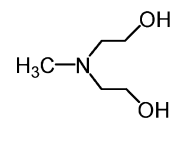

H_2L^1

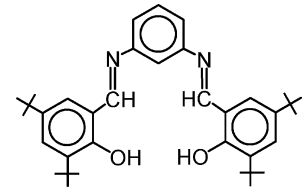

H_2L^2

The −OH (alcohol and phenol)-containing ligands have long been the ligands of choice for assembling high-

* Author to whom correspondence should be addressed. E-mail: Chaudh@mpi-muelheim.mpg.de.

(1) (a) See, for example: Crans, D. C.; Smee, J. J.; Gaidamauskas, E.; Yang, L. *Chem. Rev.* **2004**, *104*, 849. (b) Rehder, D. *Angew. Chem., Int. Ed.* **1991**, *30*, 148. (c) *Metal Ions in Biological Systems*; Sigel, H., Sigel, A., Eds.; Marcel Dekker: New York, 1995, Vol. *31*. (d) *Vanadium: The Versatile Metal*; Kustin, K., Pesssoa, J. C.; Crans, D. C., Eds.; American Chemical Society: Washington, DC, 2007; ACS Symposium Series 974. (e) Müller, A.; Peters, F.; Pope, M. T.; Gatteschi, D. *Chem. Rev.* **1998**, *98*, 849. (f) Rehder, D. *Coord. Chem. Rev.* **1999**, *182*, 297.

(2) (a) See, for example: Kaur, N.; Nellutla, S.; Dalal, S. N.; Vaid, T. P.; Cissell, J. A. *Inorg. Chem.* **2007**, *46*, 9672. (b) Krzystek, J.; Fiedler, A. T.; Sokol, J. J.; Ozarowski, A.; Zvyagin, S. A.; Brunhold, T. C.; Long, J. R.; Brunel, L.-C.; Telser, J. *Inorg. Chem.* **2004**, *43*, 5645, and references cited therein.

10.1021/ic8018327 CCC: $40.75
Published on Web 01/12/2009

nuclearity clusters[4,5] of manganese and iron, and there is no reason why the V^{III} analogues should not be accessible. Considering the oxophilicity of the vanadium center, we have used the above ligands for preparing polyvanadium complexes, which is the subject matter of this paper.

We have recently used H_2L^1 to prepare a hexadecanuclear nickel(II) complex,[6] $Ni^{II}_{16}Na^{I}_2$. The ligand H_2L^2 might additionally result in parallel spin alignment in the prepared compound through a spin-polarization mechanism, as recently reported for a ferric complex with the same ligand.[7] In this paper, we report on the extension of our studies with these two ligands, H_2L^1 and H_2L^2, and include the preparation and magnetochemical characterization of a hexanuclear vanadyl(IV) wheel

$$[Na(L^1)_6(V^{IV}{=}O)_6]ClO_4{\cdot}2CH_3OH \quad \mathbf{1}$$

and a mixed-valence tetranuclear complex

$$[(L^2)_2V^{III}_2V^{IV}_2(\mu\text{-}Cl)_6Cl_4]{\cdot}C_6H_4(NH_2)_2{\cdot}5.5(C_2H_5)_2O \quad \mathbf{2}$$

Experimental Section

Materials and Physical Measurements. Reagent- or analytical-grade materials were obtained from commercial suppliers and used without further purification. Elemental analyses (C, H, N, and metal) were performed by the Microanalytical Laboratory, Mülheim, Germany. Fourier transform IR spectra of the samples in KBr disks were recorded with a Perkin-Elmer 2000 FT-IR instrument. Electronic absorption spectra in solution were measured with a Perkin-Elmer Lambda 19 spectrophotometer. Magnetic susceptibilities of powdered samples were recorded with a SQUID magnetometer in the temperature range 2−290 K with an applied field of 1 T for **1** and **2**; complex **1** was also measured at 0.1 and 0.01 T. Experimental susceptibility data were corrected for the underlying diamagnetism using Pascal's constants and for the temperature-independent paramagnetic contributions. Mass spectra were recorded with either a Finnigan MAT 8200 (electron ionization) or a MAT 95 (electrospray ionization, ESI-MS) instrument. A Bruker DRX 400 instrument was used for NMR spectroscopy.

X-band electron paramagnetic resonance (EPR) spectra were recorded with a Bruker ELEXSYS E 500 spectrometer equipped with a helium flow cryostat (Oxford Instruments ESR 910).

Preparations. *N*′*N*-di(3,5-di-*tert*-butyl-salicylidene)-1,3-diaminobenzene, H_2L^2, was prepared as described previously.[7]

$[NaL^1_6(V{=}O)_6]ClO_4\cdot 2CH_3OH$ (1). Reaction of VCl_3 (0.32 g; 2 mmol) with *N*-methyldiethanolamine (H_2L^1; 0.24 g, 2 mmol) and $NaOCH_3$ (0.22 g, 4 mmol) in dry methanol under argon yielded a green solution, which was heated to reflux for 3 h. The solution was kept as it was for two days under an inert atmosphere, but no change was observed. Solid $NaClO_4$ (0.73 g, 6 mmol) was added to the solution, and the green color turned to blue very slowly (∼48 h). X-ray-quality deep blue crystals were obtained by slow evaporation of a methanol solution. Yield: 260 mg (∼60%; based on vanadium). Anal. calcd for $C_{32}H_{74}ClN_6NaO_{24}V_6$: C, 29.8; H, 5.8; N, 6.5; V, 23.7. Found: C, 29.5; H, 5.9; N, 6.4; V, 23.3. IR (KBr, cm^{-1}): 2865, 1645, 1567, 1459, 1075, 1037, 958, 897, 660, 585, 514. MS-ESI (pos.) in MeOH: *m*/*z* 1127.1 (100%) $[M - ClO_4]^+$. MS-ESI (neg.) in MeOH: *m*/*z* 99.1 (100%) ClO_4^-.

$[(L^2)_2V^{III}_2V^{IV}_2(\mu\text{-}Cl)_6Cl_4]\cdot C_6H_4(NH_2)_2\cdot 5.5(C_2H_5)_2O$ (2). All operations were performed under an atmosphere of argon in a glovebox. A solution of VCl_3 (0.16 g, 1 mmol) in dry THF was treated with *N*′*N*-di(3,5-di-*tert*-butyl-salicylidene)-1,3-diaminobenzene (H_2L^2; 0.54 g, 1 mmol). The resulting dark-brown solution was stirred for 1 day at ambient temperature inside the glovebox. The resulting precipitate was filtered using celite, and the filtrate was collected. From the filtrate, THF was removed in vacuo to obtain a dark-brown solid, which was recrystallized from diethylether. X-ray-quality crystals in 20% yield grew over two days. Complex **2** is very sensitive to air, so entire procedures were carried out strictly under anaerobic conditions inside the glovebox. Anal. calcd for $C_{100}H_{157}Cl_{10}N_6O_{9.5}V_4$: C, 56.0; H, 7.3; N, 3.9; V, 9.5. Found: C, 54.9; H, 7.3; N, 4.1; V, 9.3. MS-ESI (pos.) in THF: *m*/*z* 1686.9 (6%) $[M - C_4H_9]^+$, 1445.5 (11%) $[M - V_2Cl_5 - CH_9]$, 1146.6 (84%) $[M - V_2Cl_5 - C_6H_4(NH_2)_2 - C_{14}H_{33}]$, 840 (100%) $[M - V_3Cl_6 - L]$. MS-ESI (neg.) in THF: *m*/*z* 676.3 (100%) $[M - L - V_3Cl_6 - C_4H_9]$, 1282 (∼19%) $[M - C_6H_4(NH_2)_2 - 5Cl - C_5H_{12}]$. UV−vis in THF: λ_{max} (ε, M^{-1} cm^{-1}): 370 (36000), 555 (6800), 670 (5000).

X-Ray Crystallographic Data Collection and Refinement of the Structures. A dark blue single crystal of **1** and a black crystal of **2** were coated with perfluoropolyether, picked up with nylon loops, and mounted in the nitrogen cold stream of a Bruker-Nonius KappaCCD and a Bruker APEX2 diffractometer, respectively. Diffractometers were equipped with a Mo-target rotating-anode X-ray source, and graphite monochromated Mo Kα radiation (λ = 0.71073Å) was used. Final cell constants were obtained from least-squares fits of several thousand strong reflections. Intensity data of **1** were corrected using the Gaussian type method embedded in XPREP.[8a] Redundant reflection intensities were used to correct the data of compound **2** for absorption using the program SADABS.[8b]

(3) Castro, S. L.; Sun, Z.; Grant, C. M.; Bollinger, J. C.; Hendrickson, D. N.; Christou, G. *J. Am. Chem. Soc.* **1998**, *120*, 2365.

(4) (a) Selected examples: Saalfrank, R. W.; Bernt, I.; Uller, E.; Hampel, F. *Angew. Chem., Int. Ed.* **1997**, *36*, 2482. (b) Saalfrank, R. W.; Bernt, I.; Chowdhry, M. M.; Hampel, F.; Vaughan, G. B. M. *Chem.—Eur. J.* **2001**, *7*, 2765. (c) Rumberger, E. M.; Zakharov, L. N.; Rheingold, A. L.; Hendrickson, D. N. *Inorg. Chem.* **2004**, *43*, 6531. (d) Rumberger, E. M.; Shah, S. J.; Beedle, C. C.; Zakharov, L. N.; Rheingold, A. L.; Hendrickson, D. N. *Inorg. Chem.* **2005**, *44*, 2742. (e) Foguet-Albiol, D.; O'Brrrien, T. A.; Wernsdorfer, W.; Moulton, B.; Zaworotko, M. J.; Abboud, K. A.; Christou, G. *Angew. Chem., Int. Ed.* **2005**, *44*, 897. (f) Goguet-Albiol, D.; Abboud, K. A.; Christou, G. *Chem. Commun.* **2005**, *4282*. (g) Saalfrank, R. W.; Nakajima, T.; Mooren, N.; Scheurer, A.; Maid, H.; Hampel, F.; Trieflinger, C.; Daub, J. *Eur. J. Inorg. Chem.* **2005**, *1149*. (h) Saalfrank, R. W.; Scheurer, A.; Bernt, I.; Heinemann, F. W.; Postnikov, A. V.; Schünemann, V.; Trautwein, A. X.; Alam, M. S.; Rupp, H.; Müller, P. *Dalton Trans.* **2006**, *2865*.

(5) (a) See, for example: Mukherjee, S.; Weyhermüller, T.; Bothe, E.; Chaudhuri, P. *Eur. J. Inorg. Chem.* **2003**, 1956 and references therein. (b) Nihei, M.; Hoshino, N.; Ito, T.; Oshio, H. *Polyhedron* **2003**, *22*, 2359. (c) Tan, X. S.; Fujii, Y.; Nukada, R.; Mikuriya, M.; Nakano, Y. *J. Chem. Soc., Dalton Trans.* **1999**, *2415*. (d) Nolan, K. B.; Soudi, A. A. *Inorg. Chim. Acta* **1995**, *230*, 209. (e) Koikawa, M.; Yamashita, H.; Tokii, T. *Inorg. Chem. Commun.* **2003**, *6*, 157. (f) Yang, E.-C.; Harden, N.; Werrrnsdorfer, W.; Zakharov, L.; Brechin, E. K.; Rheingold, A. L.; Christou, G.; Hendrickson, D. N. *Polyhedron* **2003**, *22*, 1857. (g) Koikawa, M.; Ohba, M.; Tokii, T. *Polyhedron* **2005**, *24*, 2257. (h) Lynch, M. W.; Hendrickson, D. N.; Fritzgerald, B. J.; Pierpont, C. G. *J. Am. Chem. Soc.* **1984**, *106*, 2041. (i) Hartman, J. H.; Foxman, B. M.; Cooper, S. R. *Inorg. Chem.* **1984**, *23*, 1381. (j) Chandra, S. K.; Basu, P.; Ray, D.; Pal, S.; Chakravorthy, A. *Inorg. Chem.* **1990**, *29*, 2423, and references therein. (k) Mikuriya, M.; Shigematsu, S.; Kawano, K.; Tokii, T.; Oshio, H. *Chem. Lett.* **1990**, *729*. (l) Adam, B.; Bill, E.; Bothe, E.; Goerdt, B.; Haselhorst, G.; Hildenbrand, K.; Sokolowski, A.; Steenken, S.; Weyhermüller, T.; Wieghardt, K. *Chem.—Eur. J.* **1997**, *3*, 308.

(6) Biswas, B.; Khanra, S.; Weyhermüller, T.; Chaudhuri, P. *Chem. Commun.* **2007**, *1057*.

(7) Biswas, B.; Salunke-Gawali, S.; Weyhermüller, T.; Bachler, V.; Bill, E.; Chaudhuri, P. *Eur. J. Inorg. Chem.* **2008**, *2391*.

(8) (a) *ShelXTL 6.14*; Bruker AXS Inc.: Madison, WI, 2003. (b) *SADABS2007/4*; Bruker AXS Inc.: Madison, WI, 2007. (c) Sheldrick, G. M. *ShelXL97*; University of Göttingen: Göttingen, Germany, 1997.

Table 1. Crystallographic Data for **1** and **2**

	$1\cdot 2CH_3OH$	$2\cdot C_6H_4(NH_2)_2\cdot 5.5(C_2H_5)_2O$
chemical formula	$C_{32}H_{74}ClN_6NaO_{24}V_6$	$C_{100}H_{155}Cl_{10}N_6O_{9.5}V_4$
crystal size, mm^3	0.11 × 0.10 × 0.02	0.2 × 0.2 × 0.1
fw	1291.05	2151.56
space group	*Cc*, No. 9	$P\bar{1}$, No. 2
a, Å	13.5049(12)	15.0798(9)
b, Å	23.205(2)	20.4731(13)
c, Å	33.414(3)	22.2124(14)
α, deg	90	113.412(3)
β, deg	91.623(6)	96.194(2)
γ, deg	90	103.904(3)
V, Å	10467(2)	5947.3(6)
Z	8	2
T, K	100(2)	100(2)
ρ calcd, g cm^{-3}	1.639	1.201
reflns collected/$2\Theta_{max}$	39291/47.00	97715/50.00
unique refl./$I > 2\sigma(I)$	14982/11815	20900/12421
No. of params/restraints	1282/14	1245/226
λ, Å/*μ*(Kα), cm^{-1}	0.71073/11.70	0.71073/5.80
R1[a]/goodness of fit[b]	0.0771/1.042	0.0693/1.011
wR2[c] ($I > 2\sigma(I)$)	0.1869	0.1719
residual density, e $Å^{-3}$	+0.63/−0.61	+1.36/−0.88

[a] Observation criterion: $I > 2\sigma(I)$. $R1 = \sum||F_o| - |F_c||/\sum|F_o|$. [b] $GoF = [\sum[w(F_o^2 - F_c^2)^2]/(n - p)]^{1/2}$ [c] $wR2 = [\sum[w(F_o^2 - F_c^2)^2]/\sum[w(F_o^2)^2]]^{1/2}$, where $w = 1/\sigma^2(F_o^2) + (aP)^2 + bP$, $P = (F_o^2 + 2F_c^2)/3$.

The structures were readily solved by Patterson methods and subsequent difference Fourier techniques. The Siemens ShelXTL[8a] software package was used for solution and artwork of the structures; ShelXL97[8c] was used for the refinement. All non-hydrogen atoms were anisotropically refined, and hydrogen atoms were placed at calculated positions and refined as riding atoms with isotropic displacement parameters. Crystallographic data of the compounds are listed in Table 1.

Compound **1** was refined in noncentrosymmetric space group *Cc* (No. 9), owing two crystallographically independent complex molecules. No higher symmetry could be detected.

Two *t*-butyl groups in complex **2**, involving C69−C72 and C73−C76, were found to be disordered. A split atom model was refined, yielding occupation ratios of 0.71:0.29 and 0.57:0.43, respectively.

Three diethylether solvate molecules containing O403, O503, and O603 are also disordered. Two split positions were refined with restrained bond distances and equal anisotropic displacement parameters for corresponding disordered atoms using the SAME and EADP instructions of ShelXL97.

Results and Discussion

The synthetic procedure for **1** described in the Experimental Section yielded bright blue-colored crystalline material in good yield. A noteworthy fact is the unavailability of the cation in **1** by using other counteranions such as PF_6^-. Presumably, ClO_4^- anions act as an oxygen-transfer agent by oxidizing the V(III) precursor to a V(IV)═O unit through an abstraction of oxygen from the anion perchlorate.[9] The microanalytical results of freshly prepared **1** indicate (Experimental Section) the presence of methanol as a lattice solvent, presumably due to the comparatively strong hydrogen bonding.

The IR bands of complex **1** at 2850−2950 cm^{-1} correspond to the C−H stretches of the ligand. A moderately strong peak at 1459 cm^{-1} is attributable to the stretching of the C−N bond. The strong peak at 958 cm^{-1} is assigned to the ν(V═O) stretch, whereas medium-intensity bands at ∼600 cm^{-1} are present due to V−O−V symmetric and Na−O asymmetric stretches. The presence of the sharp bands at 1075 and 623 cm^{-1} is assigned to the ClO_4 stretching. Details of the IR peaks are given in the Experimental Section.

ESI-MS in the positive ion mode shows the monopositively charged species $[M-ClO_4]^+$ as the base peak (100%) at *m*/*z* 1127.1, whereas ClO_4^- is observed as the base peak at *m*/*z* 99.1 in ESI-MS in the negative ion mode.

The reaction of VCl_3 with H_2L^2 (1:1) in dry THF yielded a very air-sensitive solid, which was characterized as a mixed-valence tetranuclear $V^{III}_2V^{IV}_2$ species. Interestingly, X-ray structural analysis (see later) established the presence of a free *m*-phenylenediamine (1,3-diaminobenzene) molecule in the crystals of **2**. Initially, the presence of 1,3-diaminobenzene in the product was attributed to the impure ligand, as the ligand H_2L^2 had been prepared by the condensation of 1,3-diaminobenzene and 3,5-di-*tert*-butylsalicylaldehyde. Hence, the purity of the ligand (∼98.3%) was checked by chromatography (GC-MS) and other different spectroscopic and analytical methods (IR, NMR, MS, and elemental analysis), which unambiguously showed the absence of 1,3-diaminobenzene in the starting bulk material, the ligand H_2L^2. These findings led us to conclude that 1,3-diaminobenzene, present in the crystals of **2**, is generated during the complexation reaction, presumably by the phenolic proton-assisted hydrolytic decomposition of the ligand. Adventitious water might also help the hydrolysis. Moreover, only 50% of the vanadium ions (+III) got oxidized to +IV. Thus, we suggest that hydrolytic decomposition of H_2L^2 took place during the complexation reaction; reductive hydrolysis of H_2L^2 brings about the metal oxidation, V(III) to V(IV), at the cost of its own reduction. Complex **2**, like **1**, does not easily lose the solvent molecules of crystallization, as is evident from the microanalytical data.

ESI-MS in the positive and negative ion modes does not exhibit the characteristic molecular ion peak; however, peaks assignable to different fragments of complex **2** are observed and given in the Experimental Section.

The three strong electronic absorption bands of **2** in THF at 370, 555, and 670 nm are assigned, on the basis of their intensity and comparison with the corresponding diferric complex,[7] to charge-transfer transitions. Noteworthy is the absence of any band of **2** in the NIR region up to 2000 nm in different solvents like dichloromethane, diethylether, and THF.

Description of Structures. The lattice of **1** consists of discrete heptanuclear (V_6Na) monocations, perchlorate anions, and methanol molecules of crystallization. The X-ray structure confirms that a wheel-shaped hexanuclear vandyl(IV) complex has been formed with six octahedral V(IV) centers and one central sodium cation. The cyclic core, shown in

(9) (a) Taube, H. In *Mechanistic Aspects of Inorganic Reactions*; Rorabacher, C. D., Endicott, J. F., Eds.; American Chemical Society: Washington, DC, 1982; ACS Symposium Series 198, p 151. (b) Hills, E. F.; Sharp, C.; Sykes, A. G. *Inorg. Chem.* **1986**, *25*, 2566. (c) Abu-Omar, M. M.; McPherson, L. D.; Arias, J.; Béreau, V. M. *Angew. Chem., Int. Ed.* **2000**, *39*, 4310. (d) McPherson, L. D.; Drees, M.; Khan, S. I.; Strassner, T.; Abu-Omar, M. M. *Inorg. Chem.* **2004**, *43*, 4036.

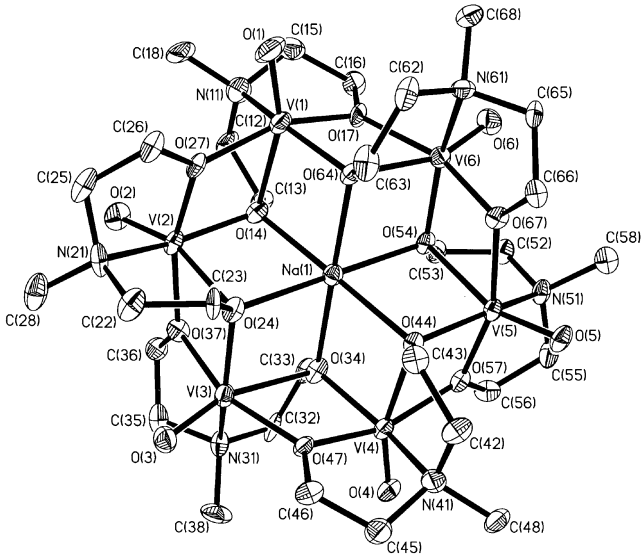

Figure 1. ORTEP drawing of **1** with thermal ellipsoids drawn at 40% probability level.

Figure 1, is comprised of a ring of six edge-sharing VO_5N octahedra linked to the central NaO_6 unit. The sodium ion located at the center of the cation forms a distorted octahedral coordination sphere from the six μ_3-O (alkoxide) atoms with the average Na−μ_3O bond distance at 2.299 ± 0.035 Å corresponding to the sum (2.33 Å) of the ionic radii of O^{2-} and Na^+.

The crystal structure of **1** thus consists of a V_6 loop with crystallographic C_i symmetry. There are two crystallographically independent molecules in the unit cell. The metrical parameters for the two molecules in the unit cell are nearly identical, and hence only one molecule is shown in Figure 1. Table 2 lists the selected bond distances and angles for **1**. The assignment of the oxidation states for the vanadium ions in **1** is relatively straightforward by examining the bond distances and the Jahn−Teller distortion expected for d^1 systems. All of the vanadium centers are six-coordinate and possess distorted octahedral geometry. The octahedral environment of each V(IV) is comprised of a terminal O atom, a N atom from the *N*-methyldiethanolamine ligand, and two

Table 2. Selected Bond Lengths (Å) and Angles (deg) of Complex **1**

V(1)···V(2)	3.276	V(2)···V(3)	3.269
V(3)···V(4)	3.275	V(4)···V(5)	3.265
V(5)···V(6)	3.295	V(6)···V(1)	3.296
Na(1)−O(14)	2.301(7)	Na(1)−O(24)	2.294(7)
Na(1)−O(34)	2.305(7)	Na(1)−O(44)	2.295(7)
Na(1)−O(54)	2.334(7)	Na(1)−O(64)	2.262(7)
V(1)−O(1)	1.620(7)	V(1)−O(17)	1.944(7)
V(1)−O(64)	1.987(7)	V(1)−O(27)	2.050(6)
V(1)−O(14)	2.197(6)	V(1)−N(11)	2.198(9)
V(2)−O(2)	1.613(7)	V(2)−O(27)	1.953(6)
V(2)−O(14)	1.992(6)	V(2)−O(37)	2.025(6)
V(2)−O(24)	2.193(6)	V(2)−N(21)	2.209(8)
V(3)−O(3)	1.616(6)	V(3)−O(37)	1.970(6)
V(3)−O(24)	2.015(6)	V(3)−O(47)	2.044(6)
V(3)−O(34)	2.204(6)	V(3)−N(31)	2.192(8)
V(4)−O(4)	1.621(6)	V(4)−O(47)	1.959(6)
V(4)−O(34)	1.992(6)	V(4)−O(57)	2.049(6)
V(4)−O(44)	2.195(6)	V(4)−N(41)	2.192(8)
V(5)−O(5)	1.626(6)	V(5)−O(57)	1.942(6)
V(5)−O(44)	1.984(5)	V(5)−O(67)	2.029(6)
V(5)−O(54)	2.219(6)	V(5)−N(51)	2.194(8)
V(6)−O(6)	1.608(7)	V(6)−O(67)	1.966(6)
V(6)−O(54)	1.997(6)	V(6)−O(17)	2.065(6)
V(6)−O(64)	2.204(6)	V(6)−N(61)	2.174(8)
O(17)−V(1)−O(27)	159.4(3)	O(27)−V(2)−O(37)	160.4(3)
O(1)−V(1)−O(14)	160.2(3)	O(2)−V(2)−O(24)	161.2(3)
O(64)−V(1)−N(11)	151.7(3)	O(14)−V(2)−N(21)	153.2(3)
O(37)−V(3)−O(47)	160.1(3)	O(47)−V(4)−O(57)	160.0(3)
O(3)−V(3)−O(34)	160.7(3)	O(4)−V(4)−O(44)	160.9(3)
O(24)−V(3)−N(31)	151.3(3)	O(34)−V(4)−N(41)	151.4(3)
O(57)−V(5)−O(67)	159.8(3)	O(67)−V(6)−O(17)	159.0(3)
O(5)−V(5)−O(54)	160.2(3)	O(6)−V(6)−O(64)	159.8(3)
O(44)−V(5)−N(51)	152.7(3)	O(54)−V(6)−N(61)	152.3(3)
V(1)−O(17)−V(6)	110.5(3)		
V(1)−O(27)−V(2)	109.8(3)		
V(2)−O(14)−V(1)	102.8(3)		
V(2)−O(37)−V(3)	109.8(3)		
V(3)−O(24)−V(2)	101.9(3)		
V(3)−O(47)−V(4)	109.8(3)		
V(3)−O(34)−V(4)	102.5(3)		
V(4)−O(57)−V(5)	109.7(3)		
V(4)−O(44)−V(5)	102.6(2)		
V(5)−O(67)−V(6)	111.1(3)		
V(5)−O(54)−V(6)	102.7(3)		
V(6)−O(64)−V(1)	103.6(3)		

μ_2-alkoxo and two μ_3-alkoxo O atoms. Both types of μ-alkoxo groups are associated with the cyclic core, and the charge balance and bond distance analysis indicate that both are deprotonated. As expected, the terminal V=O bonds are the shortest, lying in the range 1.592(6)−1.626(6) Å, whereas the V−μ_2-alkoxo(O) lengths are longer at 1.944(7)−2.065(6) Å and the V−μ_3-alkoxo(O) distances the longest at 2.208(6)−2.219(6) Å among the comparable V−O bond lengths. The V−N lengths at 2.174(8)−2.219(6) Å are in the normal range expected for a V(IV) ion.[10] Thus, all of the vanadium ions in **1** can be safely assigned to a +IV oxidation state with d^1 electronic configuration, which also corroborates with the magnetic data described later.

There is a significant amount of H-bonding between the terminal oxygens of vanadium and the proton of the MeOH solvent with the O···O separation in the range 2.746−2.760 Å. An oxygen from the counteranion perchlorate also participates in the H-bonding with the proton of the solvent molecule.

The dihedral angles between two consecutive V=O planes are approximately 70°: specifically, O(1)V(1)V(2)/O(2)V(1)-V(2), 70.3°; O(2)V(2)V(3)/O(3)V(2)V(3), 70.2°; O(3)V(3)V(4)/

(10) (a) Selected examples: Ballhausen, C. J.; Djurinsskij, B. F.; Watson, K. J. *J. Am. Chem. Soc.* **1968**, *90*, 3305. (b) Cooper, S. R.; Koh, Y. B.; Raymond, K. N. *J. Am. Chem. Soc.* **1982**, *104*, 5092. (c) Wieghardt, K.; Bossek, U.; Volckmar, K.; Swiridoff, W.; Weiss, J. *Inorg. Chem.* **1984**, *23*, 1387. (d) Kasahara, R.; Tsuchimoto, M.; Ohba, S.; Nakajima, K.; Ishida, H.; Kojima, M. *Inorg. Chem.* **1996**, *35*, 7661. (e) Plass, W. *Z. Anorg. Allg. Chem.* **1997**, *623*, 1290. (f) Salta, J.; Zubieta, J. *Inorg. Chim. Acta* **1997**, *257*, 83. (g) Vllahos, A. T.; Kabanos, T. A.; Raptopoulou, C. P.; Terzis, A. *Chem. Commun.* **1997**, *269*. (h) Kumagai, H.; Kawata, S.; Kitagawa, S.; Kanamori, K.; Okamoto, K. *Chem. Lett.* **1997**, *249*. (i) Plass, W. *Inorg. Chem.* **1997**, *36*, 2200. (j) Hamstra, B. J.; Houseman, A. L. P.; Colpas, G. J.; Kampf, J. W.; Lobrutto, R.; Frasch, W. D.; Pecoraro, V. L. *Inorg. Chem.* **1997**, *36*, 4866. (k) Soulti, K. D.; Troganis, A.; Papaioannou, A.; Kabanos, T. A.; Keramidas, A. D.; Deligiannakis, Y. G.; Raptopoulou, C. P.; Terzis, A. *Inorg. Chem.* **1998**, *37*, 6785. (l) Hagen, H.; Barbon, A.; van Faassen, E. E.; Lutz, B. T. G.; Boersma, J.; Spek, A. L.; van Koten, G. *Inorg. Chem.* **1999**, *38*, 4079. (m) Gyurcsik, B.; Jakusch, T.; Kiss, T. *J. Chem. Soc., Dalton Trans.* **2001**, *1053*. (n) Maurya, M. R.; Khurana, S.; Zhang, W.; Rehder, D. *J. Chem. Soc., Dalton Trans.* **2002**, *3015*. (o) Cashin, B.; Cunningham, D.; Daly, P.; McArdle, P.; Munroe, M.; Chonchubhair, N. N. *Inorg. Chem.* **2002**, *41*, 773. (p) Wolff, F.; Lorber, C.; Choukroun, R.; Donnadieu, B. *Eur. J. Inorg. Chem.* **2004**, *2861*.

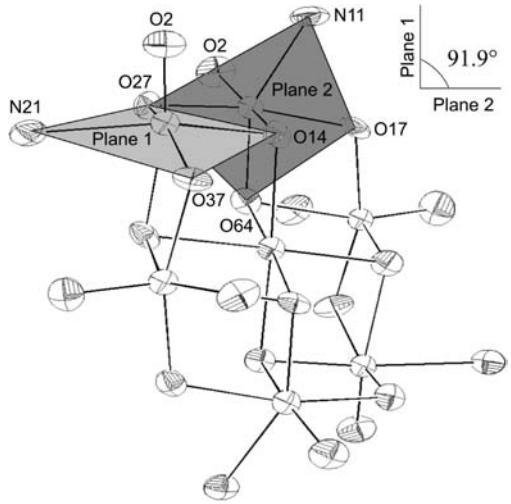

Figure 2. A side view of the core structure of **1** to emphasize the orthogonality of the neighboring *xy* planes of V(1) and V(2) atoms.

Table 3. Angles between the *xy* Planes of Two Consecutive Vanadyl Ions in **1**

plane 1	plane 2	angle between planes 1 and 2 (deg)
O(64)O(17)V(1)N(11)O(27)	O(14)O(27)V(2)N(21)O(37)	91.9
O(14)O(27)V(2)N(21)O(37)	O(24)O(37)V(3)N(31)O(47)	88.1
O(24)O(37)V(3)N(31)O(47)	O(34)O(47)V(4)N(41)O(57)	86.2
O(34)O(47)V(4)N(41)O(57)	O(44)O(57)V(5)N(51)O(67)	91.7
O(44)O(57)V(5)N(51)O(67)	O(54)O(67)V(6)N(61)O(17)	89.0
O(54)O(67)V(6)N(61)O(17)	O(64)O(17)V(1)N(11)O(27)	88.2

O(4)V(3)V(4), 69.1°; O(4)V(4)V(5)/O(5)V(4)V(5), 71.2°; O(5)V(5)V(6)/O(6)V(5)V(6), 72.6°; and O(6)V(6)V(1)/O(1)V(1)V(6), 71.1°. The angles between two consecutive *xy* planes of vanadium containing VNO_3 atoms are in the range 86.2−91.9°, one of which is shown in Figure 2. The different *xy* planes and the corresponding dihedral angles are listed in Table 3.

A very similar core $[NaV^{IV}{}_6O_6$ (triethanolamine$)_6]^+$ has been isolated[11] using the triethanolamine $(HOCH_2CH_2)_3N$ ligand. One of the three arms belonging to each of the six triethanolamine ligands projects outward from the hexagonal V_6 ring, and thus, six hydroxyl groups, in contrast to those in complex **1**, remain free from coordination to the metal ion.

The molecular geometry and atom labeling scheme of complex **2** are shown in Figure 3. Crystallographic analysis revealed that **2** contains the neutral complex $[(L^2)_2V_4(\mu\text{-}Cl)_6Cl_4]$ (Figure 3) in which an amine, 1,3-diaminobenzene, is embedded, forming H bridges to the terminal Cl atoms. Additionally, five and a half diethylether molecules are also present as a solvent of crystallization. Figure 4 exhibits embedded 1,3-diaminobenzene in the neutral complex **2**. Selected bond distances and angles for **2** are listed in Table 4.

The X-ray structure confirms that a tetranuclear vanadium complex has indeed been formed in such a way that two

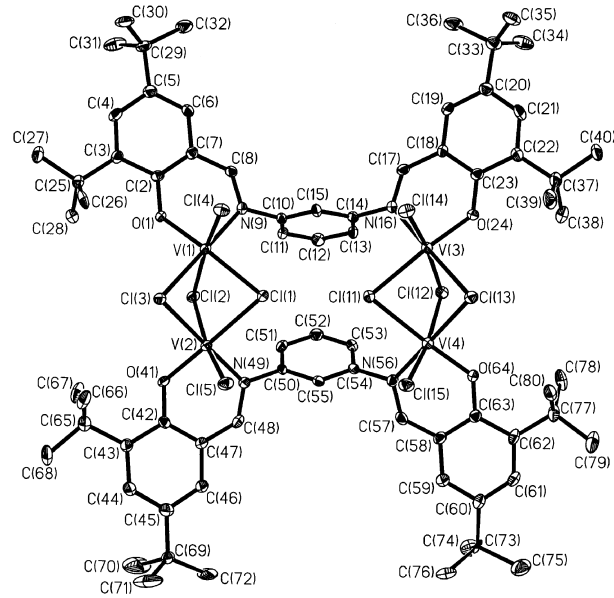

Figure 3. An ORTEP representation of **2** (40% probability).

dinuclear units, V_2Cl_5, are connected by two deprotonated $[L^2]^{2-}$ ligand anions; that is, the deprotonated ligand $[L^2]^{2-}$ acts in a binucleating fashion, with *m*-phenylene groups as linkers. The deprotonated ligand with the *m*-phenylene spacer comprising $C_{10}-C_{15}$ atoms coordinates in a bis-bidentate fashion to connect two vanadium ions, V(1) and V(3). The metrical parameters for the organic ligand are as expected and do not warrant any detailed discussion.[7] The second deprotonted ligand acts similarly to connect the V(2) and V(4) ions. The *m*-phenylene linkers are not parallel-oriented, as in the diferric complex with the same ligand.[7] The dihedral angle between the benzene planes is 51°, thus reducing significantly the possibility of face-to-face $\pi-\pi$ stacking interaction between the benzene rings of the *m*-phenylene spacers. Inspection of the bond angles at the vanadium centers indicates that the ideal trans-positioned angles are N(9)−V(1)−Cl(3) at 179.2(1)°, N(49)−V(2)−Cl(3) at 179.1(1)°, N(16)−V(3)−Cl(13) at 178.8(1)°, and N(56)−V(4)−Cl(13) at 178.6(1)°, showing that the best equatorial planes for the vanadium centers contain always deprotonated phenolate oxygens; the equatorial planes are thus V(1)O(1)Cl(1)Cl(2)Cl(4), V(2)O(41)Cl(1)Cl(2)Cl(5), V(3)O(24)Cl(11)-Cl(12)Cl(14), and V(4)O(64)Cl(11)Cl(12)Cl(15). The vanadium centers are displaced only 0.039−0.050 Å from these equatorial planes.

The coordination geometry of each vanadium ion is pseudo-octahedral, resulting from the coordination of three μ-bridged chloride ions, one terminal chloride, one phenolate oxygen, and one azomethine nitrogen atom from the ligand $[L^2]^{2-}$. The structure can be described as two face-shared octahedral units $V_2(\mu\text{-}Cl)_3$ linked to each other through two *m*-phenylene linkers. Charge balance considerations necessitate the molecule to contain two V^{III} and two V^{IV} ions; that is, complex **2** is of mixed-valence type presumably of class I according to Robin-Day classification, which is also supported by the electronic spectral measurements. The face-shared octahedral $V_2(\mu\text{-}Cl)_3$ units are known[12] for different oxidation states of vanadium, but V−Cl bond distances do

(11) (a) Khan, M. I.; Tabussum, S.; Doedens, R. J.; Golub, V. O.; O'Connor, C. J. *Inorg. Chem.* **2004**, *43*, 5850. (b) Chen, Y.; Liu, Q.; Deng, Y.; Zhu, H.; Chen, C.; Fan, H.; Liao, D.; Gao, E. *Inorg. Chem.* **2001**, *40*, 3725. (c) Thomas, C.; Li, P.; Zheng, C.; Huang, K. *Chem. Commun.* 1986, *1597*.

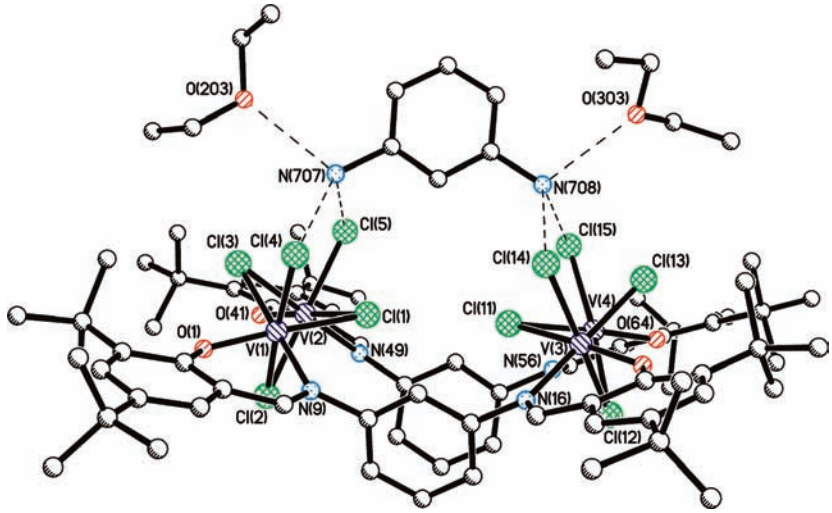

Figure 4. Molecular structure of **2** (a side view) together with embedded 1,3-diaminobenzene showing the hydrogen bondings between Cl and 1,3-diaminobenzene groups.

Table 4. Selected Bond Lengths (Å) and Angles (deg) for Complex **2**

V(1)···V(2)	3.112(1)	V(3)···V(4)	3.081(1)
V(1)···V(3)	7.084(1)	V(2)···V(4)	7.096(1)
V(1)−O(1)	1.841(3)	V(3)−O(24)	1.842(4)
V(1)−N(9)	2.084(4)	V(3)−N(16)	2.075(4)
V(1)−Cl(4)	2.360(2)	V(3)−Cl(14)	2.348(2)
V(1)−Cl(1)	2.409(1)	V(3)−Cl(11)	2.415(2)
V(1)−Cl(2)	2.457(2)	V(3)−Cl(13)	2.447(2)
V(1)−Cl(3)	2.458(2)	V(3)−Cl(12)	2.451(2)
V(2)−O(41)	1.842(4)	V(4)−O(64)	1.845(4)
V(2)−N(49)	2.061(5)	V(4)−N(56)	2.069(5)
V(2)−Cl(5)	2.370(2)	V(4)−Cl(15)	2.370(2)
V(2)−Cl(3)	2.443(2)	V(4)−Cl(11)	2.438(2)
V(2)−Cl(1)	2.446(2)	V(4)−Cl(13)	2.438(2)
V(2)−Cl(2)	2.455(1)	V(4)−Cl(12)	2.445(2)
O(1)−C(2)	1.335(6)	O(41)−C(42)	1.332(6)
C(8)−N(9)	1.286(6)	C(48)−N(49)	1.298(7)
N(9)−C(10)	1.458(7)	N(49)−C(50)	1.443(7)
N(16)−C(17)	1.292(7)	N(56)−C(57)	1.295(7)
C(23)−O(24)	1.331(6)	C(63)−O(64)	1.335(6)
O(1)−V(1)−N(9)	87.1(2)	O(24)−V(3)−N(16)	87.42(16)
O(41)−V(2)−N(49)	87.2(2)	O(64)−V(4)−N(56)	87.33(17)
V(1)−Cl(1)−V(2)	79.76(5)	V(3)−Cl(11)−V(4)	78.80(5)
V(1)−Cl(2)−V(2)	78.63(5)	V(3)−Cl(12)−V(4)	77.98(5)
V(1)−Cl(3)−V(2)	78.84(5)	V(3)−Cl(13)−V(4)	78.19(5)
N(9)−V(1)−Cl(3)	179.16(14)	N(16)−V(3)−Cl(13)	178.81(14)
Cl(4)−V(1)−Cl(2)	170.60(5)	Cl(14)−V(3)−Cl(12)	171.35(6)
O(1)−V(1)−Cl(1)	174.99(13)	O(24)−V(3)−Cl(11)	173.97(13)
N(49)−V(2)−Cl(3)	179.12(14)	N(56)−V(4)−Cl(13)	178.55(13)
Cl(5)−V(2)−Cl(2)	168.09(7)	Cl(15)−V(4)−Cl(12)	169.08(6)
O(41)−V(2)−Cl(1)	178.36(12)	O(64)−V(4)−Cl(11)	176.24(12)

not lead to any unambiguous assignment of the oxidation states. Similarly, V−O (phenoxo) and V−N (azomethine) bond distances reported in the literature[10,13] are not of much help for assignment of the oxidation states, as presumably the nonbonding d electrons are involved in the M−L bonds. However, considering the shortest bridging V−Cl distances, we tentatively assign the +IV oxidation state to V(1) and V(4) atoms but the +III state to V(2) and V(3). The localized mixed-valence nature of **2** is also in conformity with the magnetic and EPR studies.

Magnetic Properties of Complexes 1 and 2. Magnetic susceptibility data measured on a polycrystalline sample of **1** at $B = 0.01$, 0.1, and 1 T are displayed in Figure 5 as μ_{eff} per molecule versus the temperature. For these three measurements, μ_{eff} changes in a similar fashion from 290−5 K.

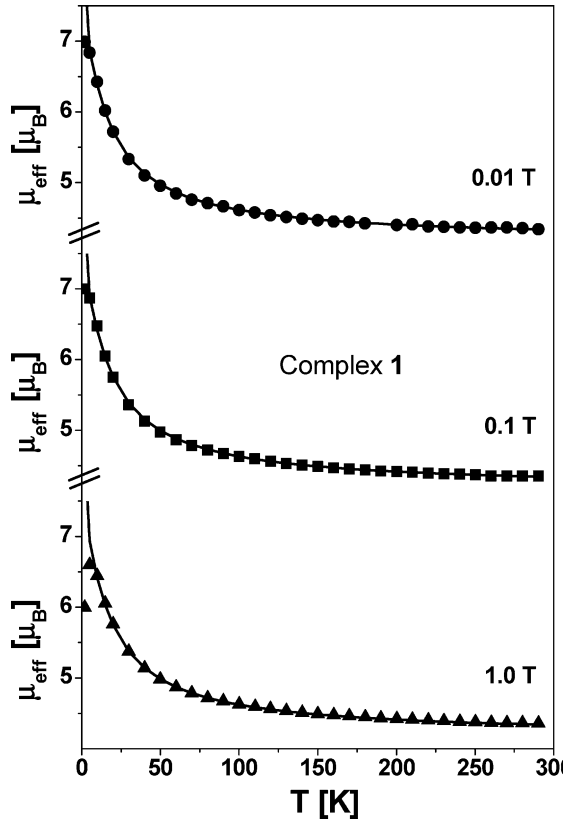

Figure 5. Plots of μ_{eff} vs T for **1** at different applied fields of 1, 0.1, and 0.01 T.

For $B = 1$ T at 290 K, μ_{eff} is equal to 4.36 μ_B($\chi_M \cdot T = 2.377$ cm^3 K mol^{-1}), which is slightly higher than 4.238 μ_B, expected for six magnetically uncoupled $S = {}^1/_2$ centers with $g = 2.0$. The μ_{eff} for **1** increases with decreasing temperature, reaching a value of $\mu_{eff} = 6.60\ \mu_B$ ($\chi_M \cdot T = 5.446$ cm^3 K mol^{-1}) at ∼5 K. Below 5 K, μ_{eff} drops to 5.99 μ ($\chi_M \cdot T = 4.491$ cm^3 K mol^{-1}) at 2 K for $B = 1$ T due to field saturation and intermolecular interactions, whereas for 2 K at $B = 0.1$ and 0.01 T, μ_{eff} increases to 7.0 μ_B ($\chi_M \cdot T = 6.123$ cm^3 K mol^{-1}). This behavior of μ_{eff} versus T at $B = 1$, 0.1, and 0.01 T is characteristic of a

Table 5. Simulated Magnetic Parameters for Complex **1**

$B(T)$	J/cm^{-1}	g	TIP (cm^3/mol)	θ (K)
1	+16.7	1.97	360.0×10^{-6}	0.205
0.1	+17.0	1.97	644.5×10^{-6}	0.074
0.01	+16.4	1.97	661.1×10^{-6}	0.070

ferromagnetic coupling between the adjacent vanadium(IV) centers with $S = {}^1/_2$within the wheel.

The Heisenberg six-atom ring model has been used to describe the experimental magnetic data, and accordingly the Hamiltonian is

$$\hat{H} = -2J\sum_{i=1}^{6} \vec{S}_i\vec{S}_{i+1} + g\mu_B\vec{B}\sum \vec{S}_i \qquad (1)$$

where S_7 is defined as S_1. The energy of the different spin states for **1** was obtained from the paper of Orbach,[14] and these values were used in van Vleck's equation to obtain the analytical expression for magnetic susceptibility for simulation of the experimental results. The Weiss constant θ was also considered to account for intermolecular interactions. The simulated curves are shown as solid lines in Figure 5, and the best fit parameters are given in Table 5. Without intermolecular interaction parameter θ, the low-temperature (2−15 K) susceptibility data could not be reproduced well. The shortest intermolecular distance is 6.30 Å, and there are two molecules in the unit cell, thus justifying the presence of intermolecular interactions. The ferromagnetic nature of the interaction can be rationalized in a straightforward way, as the interaction is determined by the $3d_{xy}$ magnetic orbital, in which the single unpaired electron (d^1, $S = {}^1/_2$) is present, where z is defined by V═O. The angles between the consecutive xy planes of vanadium with the VNO_3 atoms are near 90° (see Figure 2), thus making the magnetic orbitals orthogonal to each other, which results in ferromagnetic exchange interactions.[15] A pictorial representation of such accidental orthogonality in a wheel-shaped oxovanadium(IV) compound is shown in Figure 6. The comparatively weak interaction ($J \approx +16.7$ cm^{-1}) may be attributed to the different angles lying in the range 86.2−91.9° between the consecutive xy planes containing the VNO_3 atoms. It is interesting to note that the energy difference between the ground state ($S_t = {}^6/_2$) and the first excited state for **1** with a six-membered ring of V(IV) is $\Delta E \sim 0.5$ J, that is, ~8.4 cm^{-1}.

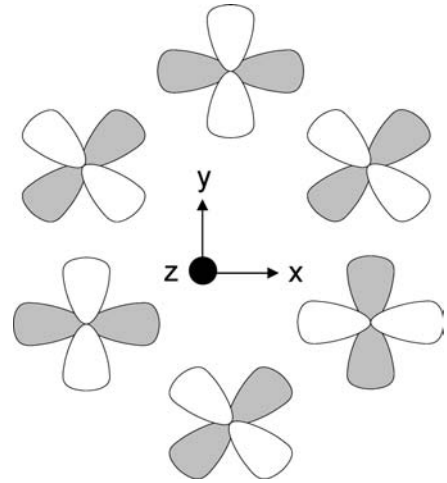

Figure 6. A pictorial representation of the orthogonal arrangement of d_{xy} orbitals of six *syn*-vanadyl sites in the V_6 ring of **1**.

Ferromagnetic interactions have also been observed for comparable [Na(V═O)$_6$(triethanolamine)$_6$][11a] and [Na(V═O)$_6$(triethanolamine)$_6$]$_2S_6$[11b] complexes, in which two arms of each triethanolamine ligand, N(CH$_2$CH$_2$OH)$_3$, are coordinated, whereas the third ligand arm, −CH$_2$CH$_2$OH, remains pendent to the hexagonal ring. The compound with the S_6^{2-} counteranions has been reported with the exchange parameter $J = +3.97$ cm^{-1},[11b] whereas for the other compound with the Cl$^-$ anion, J was found to be 19.6 K (~13.6 cm^{-1}).[11a] The low value reported for the S_6^{2-}-containing compound may be erroneous and due to the simplified model used for simulation of the experimental data.[11b] The evaluated exchange coupling parameter $J = +16.7 \pm 0.3$ cm^{-1} (Table 5) for **1** is similar to that reported for [Na(V═O)−(triethanolamine)$_6$]Cl.[11a]

To investigate the nature and magnitude of the exchange interaction propagated by the bridging chloride ligands and to examine the spin polarization effect[7,16] presumably arising from the *m*-phenylene linkage between the two $V_2(\mu\text{-Cl})_3$ units in **2**, the magnetic susceptibility data for a dried and powdered sample of **2** were collected at an applied magnetic field of 1 T and in the temperature range 2−290 K. A plot of the effective magnetic moment, μ_{eff}, versus the temperature, T, is displayed in Figure 7. The effective magnetic moment, μ_{eff}, decreases monotonically from 4.14 μ_B ($\chi_M \cdot T = 2.142$ cm^3 K mol^{-1}) at 290 K upon cooling to 2.164 μ_B ($\chi_M \cdot T = 0.586$ cm^3 K mol^{-1}) at 5 K, indicating the presence of dominating antiferromagnetic exchange coupling between the paramagnetic centers in **2**. Below 5 K, μ_{eff} drops to 1.61 μ_B at 2 K due to the combined effects of field saturation and zero-field splitting.

To avoid overparametrization, we have considered a 2J model (Scheme 1) in which the interactions between the atoms V(1)/V(3) and V(2)/V(4) propagated via the *m*-phenylene linker are taken to be equal. J_1 represents the exchange interaction between the two vanadium centers

(12) (a) Bouma, R. J.; Teuben, J. H.; Beukema, W. R.; Bansemer, R. L.; Huffman, J. C.; Caulton, K. G. *Inorg. Chem.* **1984**, *23*, 2715. (b) Cotton, F. A.; Duraj, S. A.; Roth, W. J. *Inorg. Chem.* **1985**, *24*, 913. (c) Cotton, F. A.; Duraj, S. A.; Manzer, L. E.; Roth, W. J. *J. Am. Chem. Soc.* **1985**, *107*, 3850. (d) Mazzanti, M.; Florriani, C.; Chiesi-Villa, A.; Guastino, C. *Inorg. Chem.* **1986**, *25*, 4158. (e) Mozzanti, M.; Gambarotta, S.; Florriani, C.; Chiesi-Villa, A.; Guastino, C. *Inorg. Chem.* **1986**, *25*, 2308. (f) Güdel, H.; Riesen, H. *Inorg. Chem.* **1984**, *23*, 1880. (g) Canich, J. A. M.; Cotton, F. A.; Duraj, S. A.; Roth, W. J. *Polyhedron* **1987**, *6*, 1433. (h) Calderazzo, F.; Benedetto, G. E. D.; Pampaloni, G.; Mössmer, C. M.; Strähle, J.; Wurst, K. *J. Organomet. Chem.* **1993**, *451*, 73. (i) Rambo, J. R.; Bartley, S. L.; Streib, W. E.; Christou, G. *J. Chem. Soc., Dalton Trans.* **1994**, *1813*. (j) Karet, G. B.; Castro, S. L.; Folting, K.; Bollinger, J. C.; Heintz, R. A.; Christou, G. *J. Chem. Soc., Dalton Trans.* **1998**, *67*. (k) Feghali, K.; Harding, D. J.; Reardon, D.; Gambarotta, S.; Yap, G. *Organometallics* **2002**, *21*, 968.
(13) A recent example: Graysman, S.; Goldberg, I.; Goldschmidt, Z.; Kol, M. *Inorg. Chem.* **2005**, *44*, 5073, and references therein.
(14) Orbach, R. *Phys. Rev.* **1959**, *115*, 1181.
(15) Kahn, O. *Molecular Magnetism*; VCH: New York, 1993.
(16) Ishida, T.; Mitsubori, S.; Nogami, T.; Takeda, N.; Ishikawa, M.; Iwamura, H. *Inorg. Chem.* **2001**, *40*, 7059, and references therein.

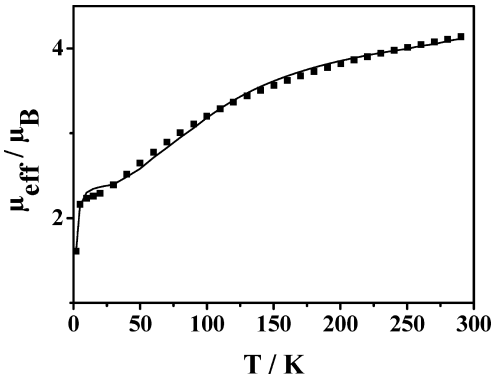

Figure 7. Temperature-dependence of the magnetic moments μ_{eff}/molecule for complex **2**.

Scheme 1

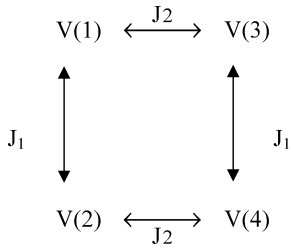

Table 6. Simulated g_i and Hyperfine Tensors for V^{III} and V^{IV} (A^{III} and A^{IV}, respectively) for Complex **2**

g_i	A^{III} (10^{-4} cm^{-1})	A^{IV} (10^{-4} cm^{-1})	g_{iso} [b]	$A^{III}{}_{iso}$ [b] (10^{-4} cm^{-1})	$A^{IV}{}_{iso}$ [b] (10^{-4} cm^{-1})
$g_x = 1.995$	45.0	−10.0			
$g_y = 1.995$	45.0	−10.0	1.987	49.2	−11.2
$g_z = 1.970$	56.7	−13.3			

[a] $g_{iso} = (\sum g_i^2/3)^{1/2}$. [b] $A_{iso} = (\sum A_i^2/3)^{1/2}$.

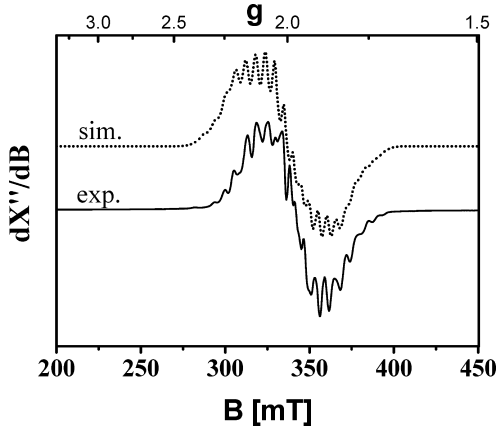

Figure 8. X-band EPR spectrum of **2**, $V^{III}{}_2V^{IV}{}_2$, in DCM at 10.9 K (experimental conditions: microwave frequency, 9.43 GHz; power, 0.25 mW; modulation amplitude, 1 mT) together with the simulated spectrum (dotted line) considering the triplet state ($S = 1$) of **2**.

[V(III)/V(IV)] mediated by the chloride bridges, whereas J_2 represents the exchange interaction between the two $V_2(\mu$-$Cl)_3$ units propagated via the *m*-phenylene spacers. The susceptibility data based on the Heisenberg spin Hamiltonian for a tetranuclear complex were simulated, shown as the solid line in Figure 7, using a least-squares fitting computer program with a full-matrix diagonalization method.[17]

$$\hat{H} = -2J_1(\vec{S}_1 \cdot \vec{S}_2 + \vec{S}_3 \cdot \vec{S}_4) - 2J_2(\vec{S}_1 \cdot \vec{S}_3 + \vec{S}_2 \cdot \vec{S}_4) \quad (2)$$

The best fit parameters obtained are $J_1 = -47.6$ cm^{-1}, $J_2 = +1.5$ cm^{-1}, $g(V^{III}) = g_1 = g_4 = 1.95$, and $g(V^{IV}) = g_2 = g_3 = 1.85$. It is to be mentioned that the quality of simulation deteriorates by considering identical "*g*" values for the different vanadium centers. The *g* value of the ground state g_t is related to local values of the individual metal ions with a spin-dependent weight factor from the Wigner−Eckart theorem; the expression[15] is $g_t = {}^4/_3 g_{V(III)} - {}^1/_3 g_{V(IV)}$. Thus, $g_t = 1.983$ calculated from the evaluated $g_{V(III)}$ and $g_{V(IV)}$ values from the magnetic data given above is in complete agreement with the g_{iso} value obtained from the simulated EPR spectrum of **2** at 10 K (see later). It is interesting to note that the Hamiltonian used does not consider any unquenched orbital momentum of V(III) ions. Noteworthy in this context is the recent report[18] of two isomeric alkoxide-bridged butterfly cores with oxidation states $[V^{III}{}_2V^{IV}{}_2]$, in which also exchange interactions are of antiferromagnetic in nature. The weak ferromagnetic interaction, $J_2 = +1.5$ cm^{-1} in **2** may be attributed to the spin polarization mechanism arising from the bridging topology (1,3 substitution of the phenylene linkers), as was observed earlier for a diferric(III) complex.[7] The energy gap between the singlet and triplet states is only about $\Delta_{S-T} = 2.5$ cm^{-1} (~3.6 K) at zero external field.

The exchange coupling parameter in the $[V^{II}{}_2(\mu\text{-}Cl)_3]^+$ core[12f] (d^3−d^3) has been determined very accurately by optical absorption to be $2J = -187 \pm 5$ cm^{-1}, whereas in comparable $(\mu$-$Cl)_3$-bridged bioctahedral species with the V^{III} ions (d^2−d^2 pair),[12i,j] the antiferromagnetic interactions as determined by variable-temperature magnetic susceptibility measurements are weaker and vary between $J = -13.4$ and $J = -48.0$ cm^{-1}. It is to be noted that inelastic neutron scattering, magnetic circular dichroism, and magnetic susceptibility studies exhibited ferromagnetic interactions within the core in $Cs_3[V^{III}{}_2Cl_9]$ and $Rb_3[V^{III}{}_2Br_9]$.[19] To deliver complex **2** in this context, keeping in mind that no mixed-valent $(\mu$-$Cl)_3$-bridged V^{III}−V^{IV} species is known, the moderate antiferromagnetic exchange parameter $J_1 = -47.6$ cm^{-1} for **2** is quite reasonable.

The X-band EPR spectrum of **2** in CH_2Cl_2 at 10 K is displayed in Figure 8. The derivative spectrum consists of multiple lines around $g \approx 2$. At the beginning, we tried to simulate the spectrum assuming $S = {}^1/_2$, arising either from mononuclear V^{IV} species originated from the tetranuclear core or due to the presence of an antiferromagnetically coupled $V^{III}V^{IV}$ (d^2d^1) dimeric unit. Both of these considerations did not yield any satisfactory simulation. Finally, the production of a similar theoretical spectrum to the experimental spectrum was achieved by considering that the

(17) Bill, E. *Julx Program*; Max-Planck-Institut für Bioanorganische Chemie: Mülheim an der Ruhr, Germany, 2005. Available from: http://ewww.mpi-muelheim.mpg.de/bac/logins/bill/julx-on.php (accessed Dec. 2008).

(18) Tidmarsh, I. S.; Scales, E.; Brearley, P. R.; Wolowska, J.; Sorace, L.; Caneschi, A.; Laye, R. H.; McInnes, E. J. L. *Inorg. Chem.* **2007**, *46*, 9743.

(19) Leuenberger, B.; Briat, B.; Canit, J. C.; Furrer, A.; Fischer, P.; Güdel, H. U. *Inorg. Chem.* **1986**, *25*, 2930.

tetranuclear vanadium core in **2** remained intact in the frozen solution. The principal fitting parameters are listed in Table 6, and the simulation along with the experimental spectrum are shown in Figure 8. The spectrum is thus analyzed with $S = 1$. The simulated hyperfine parameters A^{III}_{iso} and A^{IV}_{iso} of 49.2×10^{-4} and -11.2×10^{-4} cm^{-1}, respectively, led to a ratio A^{III}/A^{IV} of 4:−0.91, which is very similar to the theoretical ratio of 4:−1.0 expected for a $V^{III}V^{IV}$ system. Thus, the EPR spectrum is also in conformity with the notion that the mixed-valence $V^{III}V^{IV}$ species has indeed been formed, and the tetranuclear core remains intact in solution.

Concluding Remarks

We have prepared two polynuclear vanadium complexes, **1** and **2**, using alkoxide- and phenolate-based ligands. Complex **1** has been isolated in good yield, and in situ generation of vanadyl (V^{IV}═O) ions was accomplished by a presumably oxygen-atom transfer reaction induced by the perchlorate anions. The cyclic core of **1** is comprised of a ring of six edge-sharing (O═VO_4N) octahedra linked to a central Na^+ ion. Thus, the hexanuclear ring contains six vanadyl(IV) ions, in which the neighboring *xy* planes are orthogonal to each other, thus facilitating intramolecular exchange interactions to be ferromagnetic. The Heisenberg six-atom ring model ($S_i = {}^1/_2$) was successfully used to evaluate the exchange coupling parameter of $J = +16.7 \pm 0.3$ cm^{-1} from variable-temperature magnetic susceptibility measurements.

This work demonstrates that the Schiff-base ligand H_2L^2 acts as a dinucleating ligand to coordinate in a bis-bidentate fashion for stabilizing an unprecedented member of the redox family of tris-μ-chloride-bridged bioctahedral divanadium core, that is, the $V^{III}(\mu\text{-}Cl)_3V^{IV}$ unit. Additionally, the ferromagnetic coupling ($J_2 = +1.5$ cm^{-1}) operates at a distance of ~7.09 Å between two vanadium centers (d^1-d^2) through the spin polarization mechanism probably due to the topology (1,3- substitution) of the *m*-phenylene bridges.

An unexpected solvolysis of the ligand induced by the starting material VCl_3 has occurred during the complexation reaction, resulting in redox changes of vanadium ions strictly under anaerobic conditions together with the presence of uncoordinated 1,3-diaminobenzene in the crystals of **2**.

X-band EPR measurements of **2** have unambiguously proved the presence of a tetranucler mixed-valent vanadium core intact in solution. The EPR spectrum in CH_2Cl_2 at 10 K was only possible to simulate considering the triplet state ($S = 1$) of **2**, thus implying the ferromagnetic interaction between two $S = {}^1/_2$ states arising from the dominating antiferromagnetic interactions between each of the pairs V(1)/V(2) and V(3)/V(4).

Work is in progress to synthesize a ligand for studying the combined coordinating effects of alcoholic and phenolic O-donor atoms on the vanadium center in different oxidation states, which will be the subject matter of a future paper.

Acknowledgment. We thank the Max-Planck Society and the German Research Council (DFG; Priority Program "Molecular Magnetism") for funding. We also deeply appreciate the skilful technical assistance of Heike Schucht, Andreas Göbels, and Frank Reikowski.

Supporting Information Available: Crystallographic cif files for **1** and **2**. This material is available free of charge via the Internet at http://pubs.acs.org.

IC8018327